Talanta 122 (2014) 91–96

Contents lists available at ScienceDirect

Talanta

journal homepage: www.elsevier.com/locate/talanta

Fabrication of metal-organic frameworks and graphite oxide hybrid composites for solid-phase extraction and preconcentration of luteolin

Yang Wang *, Yichun Wu, Huali Ge, Huanhuan Chen, Guiqin Ye, Xiaoya Hu *

College of Chemistry and Chemical Engineering, Yangzhou University, Yangzhou 225002, China

ARTICLE INFO

Article history:
Received 31 October 2013
Received in revised form
17 January 2014
Accepted 20 January 2014
Available online 31 January 2014

Keywords:
Metal-organic frameworks
Graphite oxide
Solid-phase extraction
Luteolin

ABSTRACT

A novel solid-phase extraction sorbent, metal-organic frameworks and graphite oxide hybrid composite, was prepared by a solvothermal technique. The morphology and properties of the resultant material were examined by Fourier transform infrared spectroscopy, X-ray diffraction and field emission scanning electron microscopy. To evaluate the extraction performance of the resultant sorbent, luteolin was chosen as a model analyte. The extraction conditions were optimized. Based on these, a convenient and efficient solid-phase extraction procedure for the determination of luteolin was established and the subsequent quantification step was performed by square wave anodic stripping voltammetry. Under the optimal conditions, the oxidation current increased linearly with increasing the concentration of luteolin in the range of 5.0×10^{-9}–5.0×10^{-7} mol L^{-1} with a correlation coefficient of 0.9983 and a detection limit of 7.9×10^{-10} mol L^{-1}. The relative standard deviation of seven successive scans was 4.20% for 5.0×10^{-8} mol L^{-1} luteolin. This work not only proposes a useful method for sample pretreatment, but also reveals the great potential of metal-organic frameworks based hybrid materials as an excellent sorbent in solid-phase extraction.

1. Introduction

As one of the more common flavonoids, luteolin plays an important role in the human body. It is a frequent component of the human diet and has gained increasing interest because of its positive health effects. Luteolin has antioxidant, anti-inflammatory, anti-allergic, anticancer and immune-modulating properties to suppress hyperactive immune systems [1–3]. In clinic it is a promising agent for use in ophthalmology, cardiovascular disease, hepatitis, etc. Consequently, the development of reliable methods for the determination of luteolin is of particular significance.

So far, several methods have been investigated to determine trace amount of luteolin, such as gas chromatography [4], high-performance liquid chromatography [5] and capillary zone electrophoresis [6]. The determination of luteolin using these techniques shows high sensitivity, but they also requires expensive instruments, time-consuming pre-treatment steps, skilled operators and large quantity of organic solvents. Moreover, these techniques cannot be used for in situ assay. Electrochemical sensors show advantages of cheap instrument, simple operation and time-saving, and many electrochemical methods have been reported for luteolin sensor [7,8]. For instance, Wu et al. used a heated pencil lead disk electrode to determine luteolin in simulated human urine [9]. Franzoi et al. constructed a electrochemical biosensor for luteolin based on silver or gold nanoparticles in ionic liquid and laccase immobilized in chitosan modified with cyanuric chloride [10]. Liu et al. depicted the determination of luteolin at a glassy carbon electrode (GCE) for pharmaceutical analysis [11].

Due to low concentrations of analytes and complexity of matrices, preconcentration is usually necessary before instrumental analysis. Some extraction methods, for example, liquid–liquid extraction [12], cloud point extraction [13], and solid-phase extraction (SPE) [14,15], have been employed to extract desired organic compounds from a sample matrix. Among these techniques, SPE offers an excellent alternative to the conventional sample preparation methods because of their simplicity, consumption of small volumes of organic solvent, and ability to achieve a higher enrichment factor and sensitivity.

Metal-organic frameworks (MOFs), formed by coordination bonds between metal clusters and organic linkers, have shown significant potential for hydrogen storage, gas sorption and separation, and catalysis owing to their high specific surface areas and tunable pore sizes [16–18]. More efforts have been made to fabricate MOFs based hybrid composites for analytical applications, such as n-alkanes separation [19], lead ion sensing [20], polycyclic aromatic hydrocarbons extraction [21,22] and electrocatalytic oxidation [23]. Graphene is the most recent member of the multi-dimensional carbon-nanomaterial family. As one of the most important derivatives of graphene, graphene oxide (GO) has attracted significant

* Corresponding authors. Tel./fax: +86 514 87975587.
E-mail addresses: wangyzu@126.com (Y. Wang), xyhu@yzu.edu.cn (X. Hu).

0039-9140/$ - see front matter © 2014 Elsevier B.V. All rights reserved.
http://dx.doi.org/10.1016/j.talanta.2014.01.049

attention as a precursor of chemically converted graphene because of the advantages of large surface area, excellent conductivity and strong mechanical strength. These properties made GO as a superior candidate for solid-phase extraction [24,25]. However, the combination of metal-organic frameworks with graphene oxide ($Cu_3(BTC)_2$/GO) as a selective sorbent has not been explored until now. The purpose of this study is to examine the feasibility of $Cu_3(BTC)_2$/GO hybrid composites for the application in solid-phase extraction. Luteolin was selected as a model analyte for its potential impact on human health. The factors influencing the efficiency of solid-phase extraction were systematically studied prior to its determination with square wave voltammetry. The proposed method was successfully applied to determine luteolin in real samples and satisfactory results were obtained.

2. Experimental

2.1. Instrumentations

Electrochemical measurements were carried out with a CHI 852C electrochemical workstation (Shanghai Chenhua Instrument Company, China). A three electrode-system, with glassy carbon electrode (GCE) as the working electrode, an Ag/AgCl electrode as the reference electrode, and a platinum wire as the auxiliary electrode, were used in the measurements. All potentials were given with respect to the Ag/AgCl electrode. A Tensor 27 spectrometer (Bruker Co., Germany) was used to obtain Fourier transform infrared (FTIR) spectra. The scanning electron micrographs (SEM) images were obtained by scanning electron microscope (Hitachi S-4800, Japan). The crystalline materials were analyzed by X-ray diffraction (XRD) using a D8 Super Speed (Bruker AXS, Germany).

2.2. Reagents and materials

A 0.01 mol L^{-1} luteolin stock solution were prepared by dissolving 0.2862 g luteolin (Aladdin, Shanghai, China) in 100 mL 0.005 mol L^{-1} NaOH. Working standard solutions was obtained by step-wise dilution. Copper nitrate trihydrate ($Cu(NO_3)_2 \cdot 3H_2O$), benzene-1,3,5-tricarboxylate (BTC), and *N*, *N*-dimethylformamide (DMF) used in this work were of analytical grade and were purchased from Sinopharm Chemical Reagent Co., Ltd. (Shanghai, China) unless indicated otherwise. Phosphate buffer solution was prepared by mixing the stock solution of 0.1 mol L^{-1} NaH_2PO_4 and 0.1 mol L^{-1} Na_2HPO_4 and adjusting the pH with 0.1 mol L^{-1} H_3PO_4 or 0.1 mol L^{-1} NaOH. Graphite oxide was prepared using the Hummers method by graphite powder (Jinshan Chemicals, Shanghai, China) [26]. Double deionized water (18 MΩ cm) was prepared by Milli-Q water purification system (Millipore, Bedford, MA, USA).

2.3. Preparation of $Cu_3(BTC)_2$/GO hybrid composites

$Cu_3(BTC)_2$/GO was synthesized according to a previous report after a minor modification [27]. Briefly, $Cu(NO_3)_2$ (10 g) and H_3BTC (5 g) were dissolved in DMF (85 mL), which was stirred and sonicated for 5 min. Then, ethanol (85 mL) and deionized water (85 mL) were added to the solution in turn with stirring for 5 and 30 min, respectively. After that, GO powder (consisted of 10 wt% of the final material weight) was added to the well-dissolved MOF precursors with sonicating the resulting mixture for 30 min. Finally, the mixture was then transferred to a round-bottom flask and heated at 85 °C in an oil bath for 21 h under shaking. After cooling to ambient temperature, the products were filtered and washed several times with sufficient volume of water and ethanol and then dried at 60 °C for 6 h before use. Moreover, $Cu_3(BTC)_2$ was also prepared according to the above-mentioned procedure without the adding of GO powder for comparative analysis.

2.4. Sample extraction and preconcentration procedure

The procedure for the solid-phase extraction is as follows: a portion of 10 mL sample solution containing analyte was transferred to a beaker; the pH value was adjusted to 6 with 1 mol L^{-1} HNO_3 or 1 mol L^{-1} NaOH. Then, 15 mg of sorbent was added, and the solution was stirred for 20 min to facilitate adsorption of the luteolin onto the sorbent. After the extraction, the suspension was separated and the sorbent was shaken with 2.5 mL ethanol and phosphate buffer solution mixture (pH=5). Finally, elution solvent was transferred into an electrochemical cell for subsequent detection by square wave voltammetry.

3. Results and discussion

3.1. Characterizations of the $Cu_3(BTC)_2$/GO hybrid composites

Fig. 1 exhibits the FTIR spectra of GO, $Cu_3(BTC)_2$ and $Cu_3(BTC)_2$/GO. For GO, the FTIR spectrum indicate the presence of C=O (1725 cm^{-1}), C–O (1052 cm^{-1}), C–O–C (1223 cm^{-1}) and C–OH (1428 cm^{-1}) in the GO samples. The peak at 1615 cm^{-1} is related to a resonance peak of C–C stretching and absorbed hydroxyl groups in the GO [28]. As for $Cu_3(BTC)_2$, the peaks at 1442 and 1371 cm^{-1} are attributed to the symmetric stretching of carboxylate group in the BTC linker. The peak appeared at 1442 cm^{-1} is produced by a combination of benzene ring stretching and deformation modes, and the peak around 700 cm^{-1} is related to bending vibration of C−H. The FTIR absorption band observed at 507 cm^{-1} is assigned to a vibrational mode directly involving the Cu center [29–31]. After GO incorporation, the high intensity $Cu_3(BTC)_2$ peak swamped the characteristic GO peak due to the rather small content of GO. Hence, the FTIR spectrum of $Cu_3(BTC)_2$/GO are similar to that of $Cu_3(BTC)_2$.

Fig. 2 shows the X-ray diffraction patterns of the samples GO, $Cu_3(BTC)_2$ and $Cu_3(BTC)_2$/GO. The GO spectrum was displayed at 2θ value of 12°, which suggests that the as-prepared GO has a high degree of orientation with an interlayer distance of 7.3 Å. The diffraction pattern of $Cu_3(BTC)_2$ is in agreement with those found for well-defined $Cu_3(BTC)_2$ crystals, indicating that the current material has the expected structure [32]. The XRD patterns of GO incorporated $Cu_3(BTC)_2$ showed the same diffraction patterns as of $Cu_3(BTC)_2$, confirming that GO incorporation did not disturb or destroy the $Cu_3(BTC)_2$ crystal structure. This phenomenon is

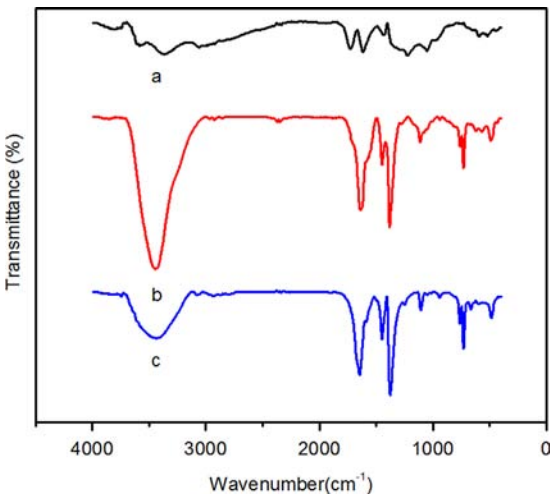

Fig. 1. FTIR spectra of (a) GO, (b) $Cu_3(BTC)_2$, and (c) $Cu_3(BTC)_2$/GO.

attributed to the exfoliation/dispersion of GO in the polar solvents used during the material preparation [29]. Moreover, based on the Scherrer equation, the size of $Cu_3(BTC)_2$/GO hybrid composite crystals was 73 nm.

SEM pictures of $Cu_3(BTC)_2$ and $Cu_3(BTC)_2$/GO are presented in Fig. 3. The SEM image of $Cu_3(BTC)_2$ was obtained as face-centered cubic crystals, demonstrating the good crystallinity of the material. The average crystal size of $Cu_3(BTC)_2$/GO was 12 μm. A significant surface roughness and several defects were observed for the $Cu_3(BTC)_2$/GO samples, indicating that the GO are indeed well admixed with $Cu_3(BTC)_2$.

3.2. Optimization of the solid-phase extraction conditions

Because the phenolic hydroxyl groups from luteolin could interface with the neighboring benzene ring through ρ–π interactions, pH could change its existing form of luteolin [33]. The effect of sample pH on the adsorption of $Cu_3(BTC)_2$/GO hybrid composites toward luteolin was studied with varying the pH from 4 to 8 and the results were presented in Fig. 4a. The results showed that the peak current increased with solution pH ranging from 4 to 6, and then the decrease of the peak current was observed when the solution pH was higher than 6. Considering the determination sensitivity, pH of 6 was chosen in the following investigation.

In order to choose the optimum amount of sorbent required for quantitative recoveries of luteolin, 5, 10, 15, 20 and 25 mg of $Cu_3(BTC)_2$/GO hybrid composites were tested and Fig. 4b showed that the signal intensity achieved by 15 mg of hybrid composites was much higher than that of by 5 and 10 mg sorbent, but almost the same with that of by 20 and 25 mg. This was because a fixed concentration and volume of sample solution was employed, which could be adsorbed completely on the surface of 15 mg hybrid composite. Although more amounts of sorbent were used, the quantity of analyte remained constant. Hence, the signal intensity kept unchanged, and 15 mg was found to be the optimum value.

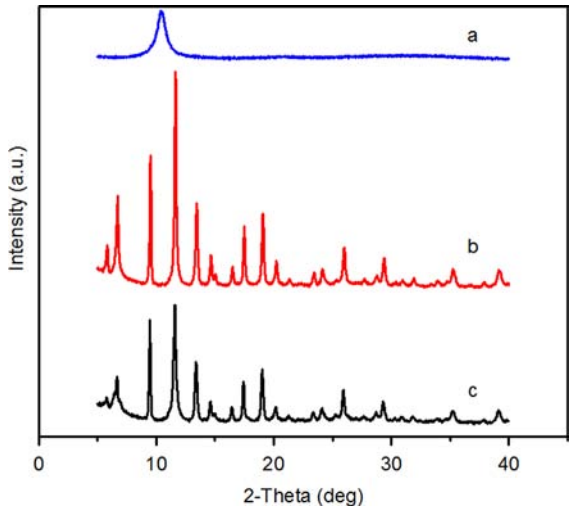

Fig. 2. X-ray diffraction patterns of (a) GO, (b) $Cu_3(BTC)_2$, and (c) $Cu_3(BTC)_2$/GO.

The amount of analyte adsorbed dependent on the rate of its mass transfer from the aqueous phase to the sorbent in the SPE procedure. Therefore, adsorption time is another important factor to be considered, and the investigation of the influence of the adsorption time was studied by varying the mixing time of $Cu_3(BTC)_2$/GO hybrid composites and sample solution from 10 to 30 min. The amount of $Cu_3(BTC)_2$/GO hybrid composites was 15 mg and it was added into 5.0×10^{-8} mol L^{-1} spiked luteolin aqueous sample. Results in Fig. 4c showed that the signal intensity increased rapidly with increased adsorption time up to 20 min, but unchanged with the adsorption time augment. Therefore, an adsorption time of 20 min was chosen for the subsequent evaluation.

The luteolin is relatively hydrophobic and a suitable organic solvent was needed to increase the desorption strength. At the same time, the luteolin oxidation occurred in the presence of acid medium, choosing a suitable elution solvent was important to ensure compatibility of the subsequent stripping procedure. In this study, eluent was prepared and optimized to achieve accurate desorption of the analytes by varying ethanol and phosphate buffer solution mixture at different volume ratios (8:2, 7.5:2.5, 7:3, 6:4 and 5:5). It was found that luteolin could be completely desorbed from the sorbent with 2.5 mL of ethanol and phosphate buffer solution mixture (6:4, v/v). The elution solvent pH of 4, 5, 6, 7 and 8 was further investigated (Fig. 4d). No lower pH value was tested, because the hybrid composites began to dissolve with a pH less than 4. The results showed that a pH of 5 was enough for subsequent work. For achieving the more efficient desorption condition, the elution time was also investigated in the range of 5–25 min with 2.5 mL elution solvent. The results showed that the signal intensity of luteolin was increased with an increase in the elution time from 5 to 15 min and kept constant up to 25. An elution time of 15 min appeared to be sufficient for complete desorption. After the first desorption, the sorbent was further desorbed with elution solvent for a second time to test the possible carryover effects. No analytes were detected after the second desorption step, indicating that the sorbent could be reused without any pretreatment.

In order to obtain the highest sensitivity and preconcentration factor, the sample volume needs to be optimized. In this case the sample solutions of 50, 100, 150, 200 and 250 mL were prepared containing fixed amounts of luteolin (5.0×10^{-8} mol L^{-1}). The signal intensity was increased with the sample volumes up to 150 mL and above this amount, it remained constant. The phenomenon could be attributed to the fact that the increase of analyte enrichment with increasing sample volume whereas a

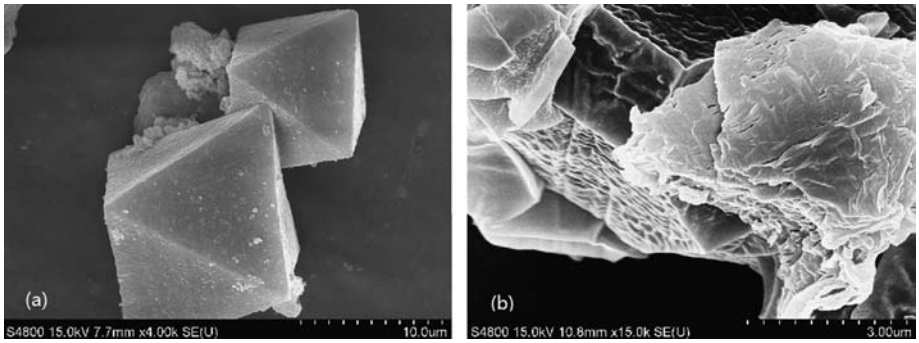

Fig. 3. SEM pictures of (a) $Cu_3(BTC)_2$ and (b) $Cu_3(BTC)_2$/GO.

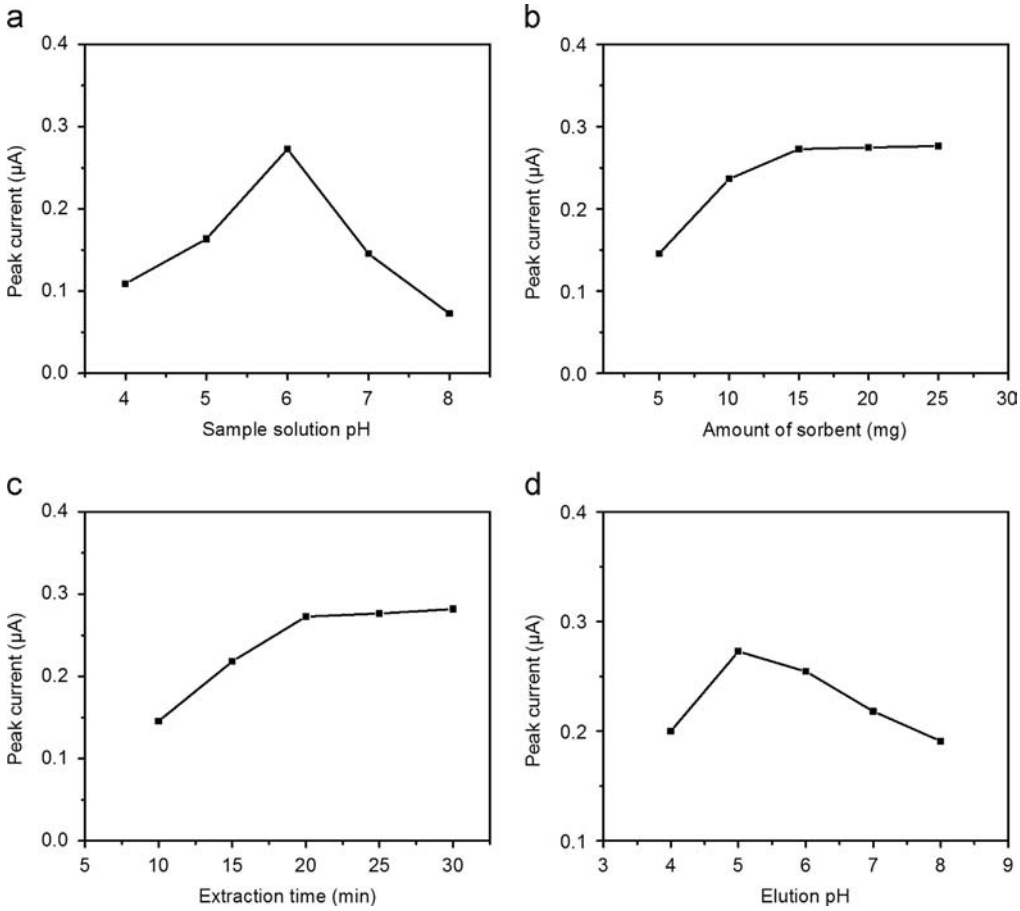

Fig. 4. Effects of (a) sample solution pH, (b) amount of sorbent, (c) adsorption time, and (d) elution pH on the peak current.

limit of this enrichment is reached when the adsorption sites are fully saturated with the analytes. Therefore, a sample volume of 150 mL was chosen as an optimum volume. The preconcentration factor is calculated from the following equation:

enrichment factor = the volume of sample/the volume of eluent

By applying of 150 mL sample volume under optimum conditions and eluting of luteolin with 2.5 mL of elution solvent, a preconcentration factor of 60 was obtained. However, for convenience, all the experiments were carried out with 10 mL of the aqueous phase.

3.3. Optimization of the determination conditions

The cyclic voltammogram of luteolin at GCE was performed between 0.1 and 0.8 V at a scan rate of 0.1 V s^{-1}. A pair of redox peaks appeared with the anodic peak potential (E_{pa}) as 0.428 V and the cathodic peak potential (E_{pc}) as 0.397 V. The anodic (I_{pa}) and cathodic (I_{pc}) peak current was obtained as 0.454 and 0.371 μA, respectively. The peak-to-peak separation (ΔE_p) was obtained as 31 mV, which is close to $2.3RT/nF$, indicating that the number of electrons involved in the reaction was $n = 1.9 \approx 2$. Cyclic voltammograms of 1.0×10^{-7} mol L^{-1} luteolin in ethanol and phosphate buffer solution mixture with different solution pH values are shown in Fig. 5. Both the reduction and oxidation peak potentials of the luteolin shifted negatively with the increase in the solution pH values. The redox peak potential of luteolin varied linearly in the range of pH values from 4 to 8 with the slope of 55 and 58 mV pH^{-1} ($E_{pa} = -0.055$ pH + 0.724, $r = 0.9956$; $E_{pc} = -0.058$ pH + 0.696, $r = 0.9994$), which was close to the theoretical value of 59 mV pH^{-1}. This result was agreement with the Nernst equation for a two-electron and two-proton transfer reaction, and the similar behavior has also been reported by Liu and co-workers [11].

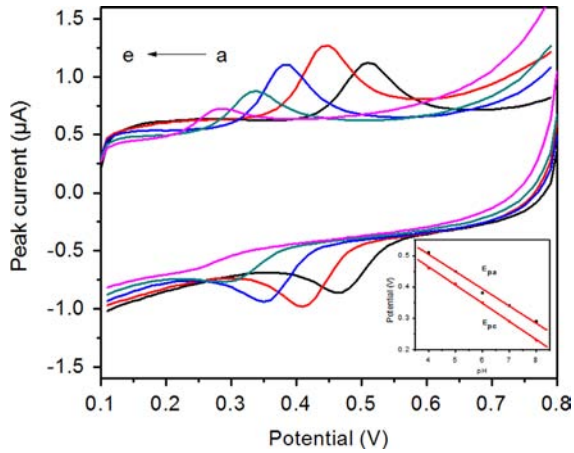

Fig. 5. Influence of buffer solution pH on cyclic voltammograms of 1.0×10^{-7} mol L^{-1} luteolin at glassy carbon electrode. Solution pH: 4, 5, 6, 7, and 8 (from a to e). Inset: Dependence of redox peak potentials on solution pH.

Fig. 6 showed the cyclic voltammograms of 1.0×10^{-7} mol L^{-1} luteolin at different scan rates. The redox peak current increased linearly with the scan rate in the range of 20–450 mV s^{-1} ($I_{pa} = 0.06225 + 0.00372v$, $r = 0.9987$; $I_{pc} = -0.08685 - 0.00278v$, $r = 0.9916$). It indicates that adsorption-controlled surface adsorption kinetics played a more important role in the electrode process. In addition, with the increase of scan rate, the E_{pa} shifted more positively and the E_{pc} shifted more negatively, indicating

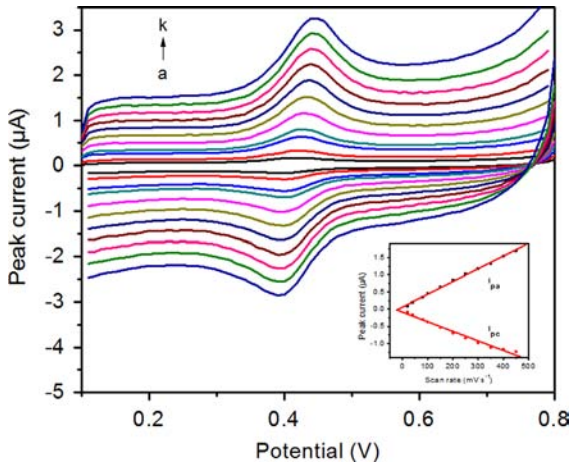

Fig. 6. Cyclic voltammograms of 1.0×10^{-7} mol L^{-1} luteolin at different scan rates (from a to k: 20, 40, 80, 100, 150, 200, 250, 300, 350, 400, and 450 mV s^{-1}.) in ethanol and phosphate buffer solution mixture (pH=5.0). Inset: Dependence of redox peak current on scan rate.

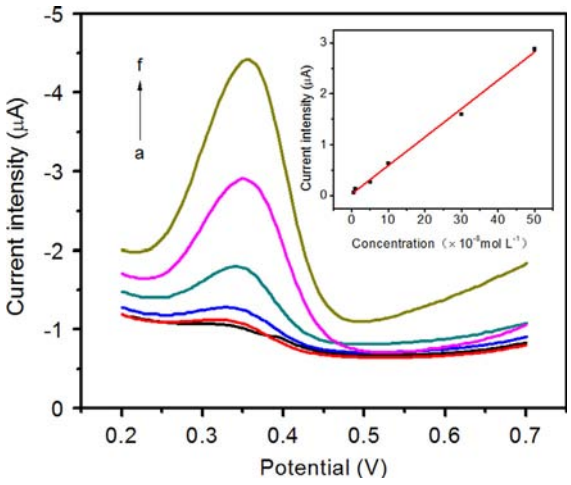

Fig. 7. Square wave voltammograms of luteolin at the following concentrations: (a) 0.5; (b) 1; (c) 5; (d) 10; (e) 30, and (f) 50×10^{-8} mol L^{-1} at step increment 4 mV, square wave amplitude 25 mV and wave frequency 25 Hz. Inset: calibration curves of luteolin.

that the electron-transfer rate decreased and the electrochemical reaction of luteolin tended to less reversible.

It was believed that accumulation can improve the amount of luteolin absorbed on the electrode surface, and then improve determination sensitivity and decrease detection limit. The accumulation under different potentials and times on the peak current was investigated. The peak current increased remarkably when the accumulation potential was increased from 0.2 to 0.4 V. However, with the further increase of the accumulation potential, the peak current decreased. Therefore, the accumulation potential was set at 0.40 V. The influence of the accumulation time on the peak current was studied at a fixed accumulation potential of 0.4 V. The current increased gradually with the accumulation time up to 300 s. With further increase of the accumulation time, the peak current increased slightly. It was probably due to the adsorptive equilibrium between the luteolin and GCE surface was saturated after 300 s. So the accumulation time is set at 300 s.

3.4. Investigation in the interferences

Prior to the application of the proposed method on real samples, it was vital to investigate the effect of some interfering ions and compounds on the signal intensity of luteolin. The adsorption and desorption of luteolin was tested in the presence of spiked known amounts of interfering species. The tolerance limit was defined as the amount of the foreign ion causing a change of $\pm$ 5% in the signal intensity. The results showed that the presence of 5-fold of quercetin and rutin; 50-fold of guanine would cause an increase in the signal intensity of luteolin, 50-fold of hypoxanthine and hesperidin would cause a decrease in the signal intensity of luteolin. The experiments also showed that 200-fold of chlorogenic acid, cysteine and dopamine; 500-fold of glucose and ascorbic acid do not interfere in the adsorption and desorption of luteolin. 1000-fold of most common matrix constituents, Na^+, K^+, Ca^{2+}, Mg^{2+}, Fe^{3+}, Cu^{2+}, NO_3^-, SO_4^{2-}, Cl^- is also tolerable. In addition, simply diluting the sample can sometimes minimize analyte matrix interference if the interferent produces no significant interference effect below a certain concentration level.

3.5. Analytical performance

Under the optimized conditions, a serial of experiments with regard to the linearity, limit of detection and repeatability were performed to validate the proposed method. Fig. 7 shows the square wave voltammogram profiles of luteolin in different concentrations and a clear oxidation peak appeared at 0.35 V. It can be seen that the anodic current increases with the luteolin concentration and a linear relationship could be established between the anodic current and the luteolin concentration in the range of 5.0×10^{-9}–5.0×10^{-7} mol L^{-1} (inset of Fig. 7). The detection limit was calculated to be 7.9×10^{-10} mol L^{-1}, which was defined as LOD=$3\sigma/s$, where σ is the standard deviation of the blank signals and s is the slope of the linear calibration graph. The repeatability of the method was evaluated and the relative standard deviation towards a 5.0×10^{-8} mol L^{-1} of luteolin solution was 4.20% for six successive assays. Moreover, the hybrid composites exhibited good stability under the experimental conditions, which could be used for more than 30 experiments without any loss in its sorption behavior. Table 1 lists the linear ranges and detection limits for luteolin determination using different analytical methods, including HPLC, CE and electrochemical methods with modified electrodes. It can be observed that the detection limit of the proposed method is lower than or comparable with the results of previous studies [5–11,33]. Accordingly, the proposed method showed a very good sensitivity, high enrichment factor and low detection limits. The sorption processes between luteolin and $Cu_3(BTC)_2$/GO can be attributed to the fact that luteolin molecules can penetrate into the $Cu_3(BTC)_2$/GO channel, and the shape and size of the pores lead to shape- and size-selectivity over the guests which may be adsorbed. Another important factor for this behavior is primarily through the hydrophobic and π–π stacking interactions between luteolin and $Cu_3(BTC)_2$/GO hybrid composites.

3.6. Analytical applications

The performance of the proposed method was tested by analyzing tablets and chrysanthemum tea samples. The tablet and chrysanthemum tea were purchased from local Chinese pharmacy store and finely pulverized by electric blender before the experiment. 0.5 g of powdered samples was transferred into a beaker together with 10 mL ethanol for 20 min with the aid of ultrasonication. After being filtered through a filter paper, the extract was diluted to 50 mL conical beaker with ethanol, and then the contents of luteolin were analyzed after appropriate dilution. All samples obtained were analyzed in three replicates. The results are outlined in Table 2 with the recoveries between 97.0 and

Table 1
Comparison of analytical properties for the determination of luteolin.

Methods	Linear range (μmol L^{-1})	Detection limit (μmol L^{-1})	Ref.
High-performance liquid chromatography	0.31–89	0.070	5
Capillary zone electrophoresis	6.60–528	0.45	6
Differential pulse voltammetry using multiwalled carbon nanotubes modified glassy carbon electrode	0.0002–0.003	0.00006	7
Differential pulse voltammetry using macroporous carbon modified glassy carbon electrode	0.3–30	0.0013	8
Square wave voltammetry using heated pencil lead disk electrode	0.004–1	0.001	9
Square wave voltammetry using Ag or Au nanoparticles dispersed in BMI · PF_6	0.099–5.825	0.054	10
Differential pulse voltammetry using glassy carbon electrode	0.01–1	0.005	11
Liquid phase microextraction combined with high-performance liquid chromatography	0.01–1.75	0.00175	33
Square wave voltammetry combined with solid-phase extraction	0.005–0.5	0.00079	This work

Table 2
Analytical results of real samples (mean ± S.D., $n=3$).

Sample	Original (mg g^{-1})	Added (mg g^{-1})	Found (mg g^{-1})	HPLC (mg g^{-1})	Recovery (%)
Tablet	2.66 ± 0.13	0.5	3.17 ± 0.15	2.61 ± 0.08	102.0
		1	3.63 ± 0.18		97.0
Chrysanthemum tea	0.310 ± 0.03	0.5	0.807 ± 0.02	0.315 ± 0.01	99.4
		1	1.32 ± 0.05		101.0

102.0%. To further evaluate the accuracy of the proposed method, the conventional HPLC method was also adopted to analyze the real samples for comparison. For HPLC analysis, the sample solutions were analyzed under the following conditions: Methanol-phosphoric acid (0.4%) (55: 45, v/v) was used as the mobile phase at a flow rate of 1 mL min^{-1}; UV detector wavelength was set at 350 nm; and sample injection was 20 μL. The peak retention time for the elution of luteolin was 8.0 min. The results obtained showed that there was no obvious difference between these two methods.

4. Conclusions

In this study, a novel $Cu_3(BTC)_2$/GO hybrid composites was synthesized, and used as an extraction media for the separation and enrichment of luteolin. The experimental results showed that hybrid composites had good adsorption capacity for target analytes, and the developed SPE exhibited many merits for the enrichment. The optimal method had attained acceptable analysis results of tablets and chrysanthemum tea samples with a little amount of sorbents with detection by square wave voltammetry. The feasibility of this method would considerably expand the application of metal-organic frameworks based composites and become a cost effective and useful extraction tool in analytical chemistry.

Acknowledgments

This work was supported by the National Natural Science Foundation of China (21205103, 21275124), Jiangsu Provincial Nature Foundation of China (BK2012258), and a Project Funded by the Priority Academic Program Development of Jiangsu Higher Education Institutions.

References

[1] K. Shimoi, N. Saka, K. Kaji, R. Nozawa, N. Kinae, BioFactors 12 (2000) 181–186.
[2] P.G. Pietta, J. Nat. Prod. 63 (2000) 1035–1042.
[3] H. Cheong, S.Y. Ryu, M.H. Oak, S.H. Cheon, G.S. Yoo, K.M. Kim, Arch. Pharm. Res. 21 (1998) 478–480.
[4] Z. Füzfai, I. Molnár-Perl, J. Chromatogr. A 1149 (2007) 88–101.
[5] J. Wu, H. Xing, D. Tang, Y. Gao, X. Yin, Q. Du, X. Jiang, D. Yang, Acta Chromatogr. 24 (2012) 627–642.
[6] Y.Y. Li, Q.F. Zhang, H.Y. Sun, N.K. Cheung, H.Y. Cheung, Talanta 105 (2013) 393–402.
[7] D.M. Zhao, X.H. Zhang, L.J. Feng, Q. Qi, S.F. Wang, Food Chem. 127 (2011) 694–698.
[8] L.J. Zeng, Y.F. Zhang, H. Wang, L.P. Guo, Anal. Methods 5 (2013) 3365–3370.
[9] S.H. Wu, B.J. Zhu, Z.X. Huang, J.J. Sun, Electrochem. Commun. 28 (2013) 47–50.
[10] A.C. Franzoi, I.C. Vieira, J. Dupont, C.W. Scheeren, L.F. de Oliveira, Analyst 134 (2009) 2320–2328.
[11] A.L. Liu, S.B. Zhang, L.Y. Huang, Y.Y. Cao, H. Yao, W. Chen, X.H. Lin, Chem. Pharm. Bull. 56 (2008) 745–748.
[12] M.A. Farajzadeh, L. Khoshmaram, Food Chem. 141 (2013) 1881–1887.
[13] E. Katsoyannos, O. Gortzi, A. Chatzilazarou, V. Athanasiadis, J. Tsaknis, S. Lalas, J. Sep. Sci. 35 (2012) 2665–2670.
[14] T. Tagami, A. Takeda, A. Asada, A. Aoyama, T. Doi, M. Kawaguchi, K. Kajimura, Y. Sawabe, H. Obana, K. Yamasaki, J. Nat. Med. 67 (2013) 838–843.
[15] F.J. Lara, M. del Olmo-Iruela, A.M. García-Campaña, J. Chromatogr. A 1310 (2013) 91–97.
[16] L. Bromberg, X. Su, T.A. Hatton, ACS Appl. Mater. Interfaces 5 (2013) 5468–5477.
[17] D.F. Liu, Y.S. Lin, Z. Li, H.X. Xi, Chem. Eng. Sci. 98 (2013) 246–254.
[18] P. Pachfule, R. Banerjee, Cryst. Growth Des. 11 (2011) 5176–5181.
[19] N. Chang, Z.Y. Gu, H.F. Wang, X.P. Yan, Anal. Chem. 83 (2011) 7094–7101.
[20] Y. Wang, Y.C. Wu, J. Xie, H.L. Ge, X.Y. Hu, Analyst 138 (2013) 5113–5120.
[21] S.H. Huo, X.P. Yan, Analyst 137 (2012) 3445–3451.
[22] X.F. Chen, H. Zang, X. Wang, J.G. Cheng, R.S. Zhao, C.G. Cheng, X.Q. Lu, Analyst 137 (2012) 5411–5419.
[23] H. Hosseini, H. Ahmar, A. Dehghani, A. Bagheri, A.R. Fakhari, M.M. Amini, Electrochim. Acta 88 (2013) 301–309.
[24] H. Tabani, A.R. Fakhari, A. Shahsavani, M. Behbahani, M. Salarian, A. Bagheri, S. Nojavan, J. Chromatogr. A 1300 (2013) 227–235.
[25] Q. Han, Z.H. Wang, J.F. Xia, S. Chen, X.Q. Zhang, M.Y. Ding, Talanta 101 (2012) 388–395.
[26] W.S. Hummers, R.E. Offeman, J. Am. Chem. Soc. 80 (1958) 1339.
[27] C. Petit, L.L. Huang, J. Jagiello, J. Kenvin, K.E. Gubbins, T.J. Bandosz, Langmuir 27 (2011) 13043–13051.
[28] G. Venugopal, K. Krishnamoorthy, R. Mohan, S.J. Kim, Mater. Chem. Phys. 132 (2012) 29–33.
[29] T.J. Bandosz, C. Petit, Adsorption 17 (2011) 5–16.
[30] R. Senthil Kumar, S. Senthil Kumar, M. Anbu Kulandainathan, Microporous Mesoporous Mater. 168 (2013) 57–64.
[31] A. Grzech, J. Yang, T.J. Dingemans, S. Srinivasan, P.C. M.M. Magusin, F.M. Mulder, J. Phys. Chem. C 115 (2011) 21521–21525.
[32] P. Chowdhury, C. Bikkina, D. Meister, F. Dreisbach, S. Gumma, Microporous Mesoporous Mater. 117 (2009) 406–413.
[33] M. Hadjmohammadi, H. Karimiyan, V. Sharifi, Food Chem. 141 (2013) 731–735.